



# USING FLOATING-INTERLEAVING BOOST CONVERTERS FOR SMALL WIND ENERGY CONVERSION

Moncef Justin Lalou

College of Engineering and Architecture Fribourg, University of Applied Sciences HES-SO, Fribourg, Switzerland, moncef.lalou@hefr.ch, ORCID: 0000-0002-7058-6487

Capone Michele

Former colleague, College of Engineering and Architecture Fribourg, University of Applied Sciences HES-SO, Fribourg, Switzerland, capomichelene@gmail.com, ORCID: 0000-0002-5654-6972

Cite this paper as: *Moncef J., Lalou. Using floating-interleaving boost converters for small wind energy conversion. 8<sup>th</sup> Eur. Conf. Ren. Energy Sys. 24-25 August 2020, Istanbul, Turkey.*

**Abstract:** Small Wind Energy Conversion System (SWECS), based on two back-to-back voltage source converters (VSC), with transformerless power injection into the utility grid, prove to be quite effective and reliable, but its efficiency and the compactness of its implementation can be improved. For this purpose, a modified topology, by introducing a floating-interleaving boost converter (FIBC), is proposed and evaluated.

In this paper, theoretical and practical aspects related to the development of a FIBC dedicated to small wind power conversion, are presented. For a given rated values of power and voltage at the injection point into the grid, and a range of generator voltage, a FIBC converter is selected and sized, then realized and tested in stand alone operation and as element of a SWECS prototype. Experimental results confirm the suitability of the modified topology to achieve a very high efficiency of the wind energy conversion.

**Keywords:** *Small wind energy, boost converter, FIBC, SWECS, efficiency.*

© 2020 Published by ECRES

## 1. INTRODUCTION

Over the last years, wind energy has been pursuing its worldwide growth as primary source of the electrical grid. With public incentive, massive investments in new plants and technologies made it possible to strongly increase the installed power capacity. Whereas this performance results mainly from large on and off-shore wind farms, we see a parallel development of small wind turbines – object of this study - whose power is rated up to approximately 10 kW, and dedicated to off-grid electrification or to locally supply the distribution grid.

As it widely reported, for instance in [4,5], the standard solution of a SWECS consists in a three phase, multipolar permanent magnet synchronous generator (PMSG), which is directly driven by the small wind turbine, and whose stator phases are connected to two VSCs (Voltage Source Converters) in back to back topology. These serves to adapt the PMSG three phase voltage with variable frequency and amplitude to those of the utility grid, while allowing to operate at maximum power point (MPP). The grid side inverter (VSI) is normally connected to the power injection point through a current harmonic filter, usually of LCL type [6].

This configuration enables full control over active/reactive powers in transit from the generator and into the grid, with control decoupling of the two converters thank to the DC-link capacitor, but has the drawbacks to generate pronounced losses with its numerous hard switching commutators (2 VSCs), and shows a heavy and cumbersome DC-link capacitor which increases costs and reduces the lifetime of the system.

In an attempt to overcome these drawbacks, the idea is to replace the generator side rectifier (VSR) by a diode rectifier in series with a boost converter (BC) of suitable properties (figure 1) in terms of efficiency, voltage ratio and compactness. To this end, the main purpose of this study is to introduce and evaluate a BC of the family of floating- interleaving boost converters (FIBCs). The same converter was successfully used, under similar requirements, to elevate Fuel Cell output voltage in an electric vehicle drive [1].

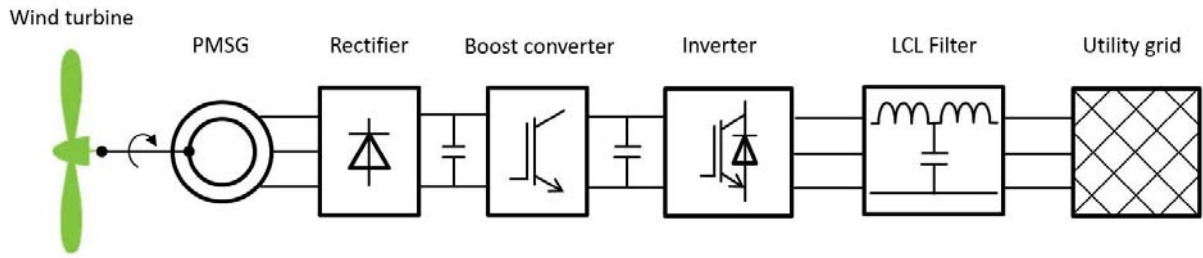


Figure 1: Structure of the SWECS.

In the following, the topology of the FIBC is first determined, and its electrical components sized by considering the rated power and input/output voltage levels. Then the necessary operating controls are performed for the FIBC and the VSI. The control of the FIBC output voltage and its inner phases currents controls, are first performed, then the control of active (and reactive) power at the grid injection point. Finally, the experimental data is collected for the FIBC operating in stand alone, and as part of the SWECS prototype, hence enabling to assess real performance of the proposed topology.

## 2. FIBC SELECTION AND CONTROL

Basically, a BC from the FIBCs family consists of a set of  $N$  conventional BC, which are shared into two groups of  $N/2$  conventional BC mounted in parallel and whose outputs are connected in series. Figure 2 gives an illustration of a quadriphase FIBC ( $N=4$ ). This topology results naturally in a higher voltage amplification capacity than the conventional BC, and in a reduced voltage and current of the passive components, as well as switching devices, thus decreasing their size and weight. Moreover, the control signals of the  $N$  switches, according to PWM control method, are shifted by an angle of  $360/N$  degree in respect to each other, which leads to lower the input currents ripple.

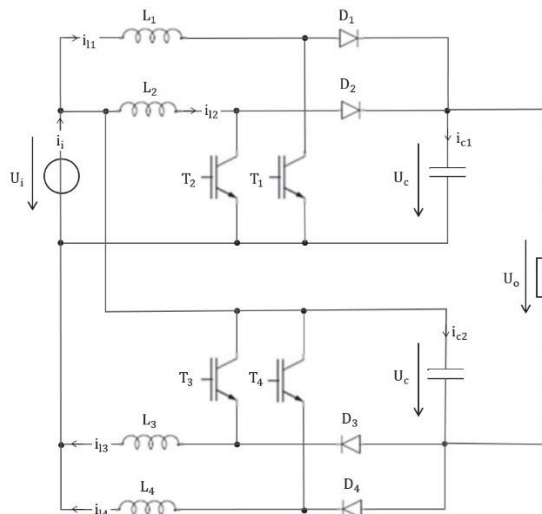


Figure 2: Four phases FIBC topology with ohmic load.

But the most relevant advantage for wind energy harvesting is an improved intrinsic efficiency, as shown in [1] through analytical comparison of power losses between the conventional BC and the FIBC for  $N=2,4,6$ , at a rated power of 5 kW and an output voltage of 400 V. From this study, it comes notably that the FIBCs with  $N=4, 6$  remains at high levels of efficiency (above 90%) over a wide range of input current, while it decreases sharply for  $N=2$  and even more with the conventional converter. The FIBC converter is therefore selected to elevate DC voltage delivered by the generator and a diode rectifier, with  $N=4$  (see figure 2) as it's proven that it detains the best tradeoff between efficiency and number of phases i.e. the complexity [1].

For a proper operation of the VSI, the output of the FIBC (i.e. DC-link) is controlled at constant voltage, depending on the rated AC voltage of the utility grid. In order to improve the dynamic behaviour of the control loop and to guarantee a balanced power sharing between the four phases, the currents are also controlled, obviously at the same reference. Due to the intrinsic switching operation of each phase, it's appropriate to use a sliding mode controller, which is known to be very robust in face of input voltage variations and output power [1].

The corresponding control scheme is given – for each phase - in figure 3, where the common current set value ( $i_{1c}$ ) is delivered by the voltage controller.

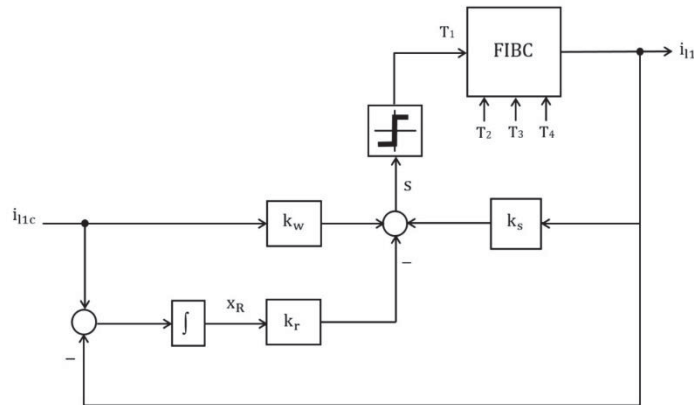


Figure 3: Sliding mode current controller scheme (phase 1).

In a similar fashion to the classical state control, the overall control results from three contributions : feedforward (gain  $k_w$ ), integral (gain  $k_r$ ) and feedback (gain  $k_s$ ). In sliding mode operation at constant PWM frequency, the average switching control ( $\bar{T}_i$ ) of a switch  $i$  ( $i=1$  to 4) is derived from the general formula given in [2, p. 21] :

$$\bar{T}_i = \frac{u_{ou} - u_{in} + A_k (i_{ref} - i_i) + B_k d(i_{ref})/dt}{u_{ou} + u_{in}}$$

This result involves the upper ( $u_{ou}$ ) and lower ( $u_{in}$ ) values of the switching control  $T_i$ , the reference ( $i_{ref}$ ) and the real value ( $i_i$ ) of the phase current, as well as two parameters :  $A_k=2 \cdot L_i \cdot k_r/k_s$ ,  $B_k=2 \cdot L_i \cdot k_w/k_s$  where  $L_i$  denotes the phase inductance. Normally, these two parameters are analytically determined through pole placement method, in sliding mode operation. But in this case, both cannot be loosely assigned since the state model of a phase current shows a nul state matrix. The two parameters were then adjusted in results-oriented manner using an appropriate simulator in Matlab/Simulink environment (see Experimental setup section). Furthermore, the PI, parallel form, DC-link voltage controller is designed using pole placement method on the basis of the transfer functions of the output voltage with respect to PWM duty cycle [3].

### 3. CONTROL AND OPERATION OF THE SWECS

In order to enable conversion at maximum power point (MPP), the generator speed is controlled, with a reference depending on the wind speed and the turbine blades features, in accordance with the tip speed ratio method. For this purpose, the active power at the injection point serves as control variable, which in turn, is controlled through the VSI (as well as the reactive power). Simultaneously, the DC-link voltage is also controlled at a sufficient level, given the grid voltage to guarantee the normal operation of the VSI.

Figure 4 gives a comprehensive description of the SWECS control scheme, where the key elements are two dual PI/P controllers that are operating simultaneously to control the grid currents ( $i_d$ ,  $i_q$ ) in Park domain. The references of these two currents are calculated according to the respective power references and grid voltage, which is assumed to be constant. For each current, a parallel form PI controller outputs the reference of the corresponding LCL filter capacitive current. Le latter is in turn subject to a P control with feedforward compensations dedicated at dynamic decoupling of  $i_d$  and  $i_q$ . The parameters of the two controllers are optimised by shaping of the open loop transfer function of  $i_d$ ,  $i_q$ , according to the methodology described in [7]. The P gain ( $k_{p2}$ ) is set to reach a loop damping factor of 0.95, and the PI parameters ( $k_{p1}$ ,  $k_{i1}$ ) to impose a phase margin of 30°.

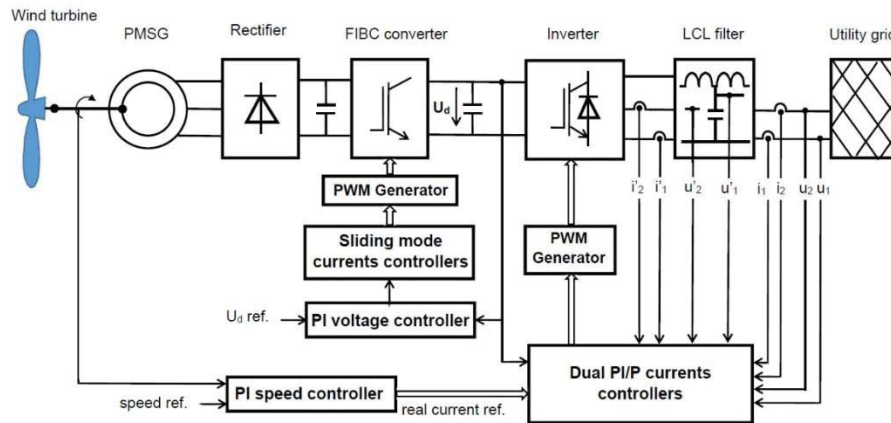


Figure 4: Control structure of the SWECS.

#### 4. EXPERIMENTAL SETUP

A prototype is developed in the aim to assess the operating performance of the proposed SWECS. The objective is to estimate efficiency of the power electronics conversion (from the generator to the grid), and to observe the behaviour of FIBC and VSI controls. For this purpose, the subsystem from the wind turbine up to the FIBC input is simply replaced by a variable DC voltage source.

The following rated values have been set : apparent injected power : 5 kVA, grid AC line voltage : 400 V, DC-Link voltage : 700 V, and the DC input range of the FIBC is assumed to vary in a relatively wide interval [100..400] V, which leads a transfer ratio within the range [1.75..7]. These settings will enable to specify the FIBC, the VSI and the LCL filter, for PWM switching frequencies of 20 kHz (FIBC) and 10 kHz (VSI).

The passive elements of the FIBC are specified to largely comply with input/output settings, and also to enable a low input current ripple to protect the generator windings. The actual specifications are optimised as trade-off between the volume clutter, cost and performance, which leads to the following specifications : inductors : 4x5mH, 6 Adc, 1.5 App @ 20 kHz, and electrolytic capacitors : 4x 4.7 mF, 400 Vdc, 4x18k $\Omega$  voltage balancing resistors. The active elements of the FIBC consists in two IGBT bridge modules 1200 V MiniSKiiP IPM with their evaluation boards. Figure 5 illustrate the FIBC assembly, which is tightened in a 16-inch rack in order to cut electromagnetic radiation due to lead wires.

Furthermore, the passive elements of the LCL filter are specified according to the design methodology detailed in [6], dedicated to low scale energy conversion systems, which leads to the following specifications :  $L_1=10$  mH (VSI side);  $L_2=2.5$  mH,  $C=2$   $\mu$ F in series with a damping resistance  $R_f=10.7$   $\Omega$ .

The remaining elements of the SWECS prototype consist in a fully integrated VSI (Semikron SkiP 25AC), two proprietary TMS 320 based DSP boards for the FIBC and the VSI controls implementation, current and voltage sensors with related signal acquisition electronics (see figure 4).

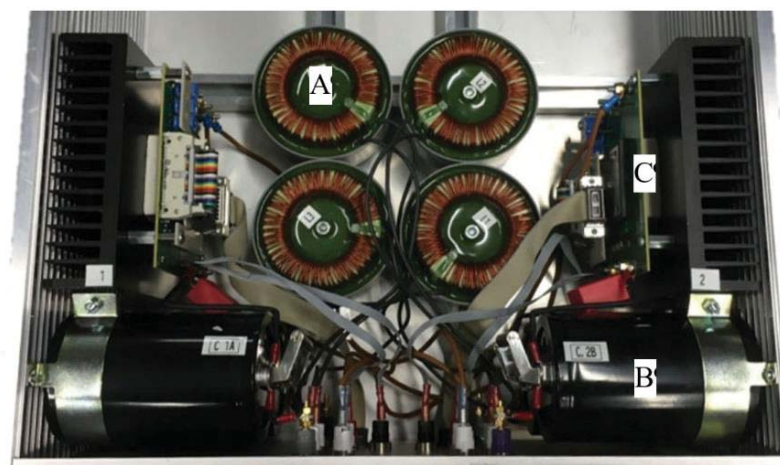


Figure 5: Four-phase FIBC prototype : A: inductor (5 mH), B: electrolytic capacitors (4.7 mF), C: IGBT module with cooler.

## 5. EXPERIMENTAL RESULTS

In a first step, the FIBC was tested in stand-alone mode, with a voltage source of 10 A/400 V as input, and as load a variable power resistor (20..400  $\Omega$ ). Figure 6 displays the four phases currents responses ( $i_{11}$  to  $i_{14}$ ) to a common reference value of 3 A ( $I_{\text{ref}}$ ).

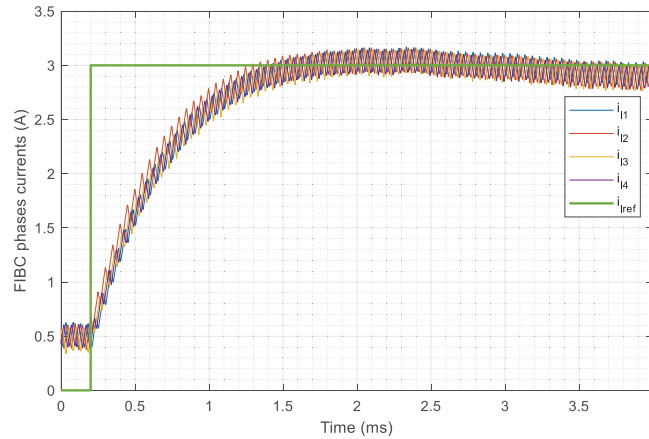


Figure 6: Responses of the FIBC's four phases currents.

The parameters  $A_k$  and  $B_k$  of the sliding mode controller were adjusted in numerical simulation using Matlab/Simulink, and thereafter fine tuned in the real setup, which results in the following values :  $A_k=20$ ,  $B_k=0$ . It can be observed a settling time of ca 1.3 ms, and almost no overshoot, while a moderate current ripple of ca 8% is recorded in steady state.

The same setup serves to test the PI control of the FIBC's output (DC-link) voltage, whose proportional ( $k_p=0.047$ ) and integral ( $k_i=7.2$ ) gains were first computed using pole placement method, then experimentally refined in results-oriented approach.

Figure 7 displays I/O measurements of the FIBC, with DC-link reference at 700 V and  $V_{\text{in}}$  at 145 V. In this case, corresponding to a relatively high transfer ratio, an output mean value of 685 V with 15 V ripple is recorded. Transitorily, the three output signals show a settling time of ca 200 ms, with almost no overshoot. In addition, FIBC experimental efficiency is determined for several input voltage values, covering the range [100..400] V. For this, input and output powers are calculated in a scope (LeCroy 44Xi) as rms values over 200 ms of instantaneous power measurements, which leads to efficiency ranging from 96% to 98 %. This result, which stresses extremely low power losses in the FIBC, is slightly higher than the one obtained in [1] with the same rated power (5 kW) and the same switching frequency (20 kHz), which is clearly expected since the duty cycle in [1] (0.7) is toward the upper limit in this case (0.75, corresponding  $V_{\text{in}}=400$  V), and the input current in [1] is much higher (70 versus 10 A).

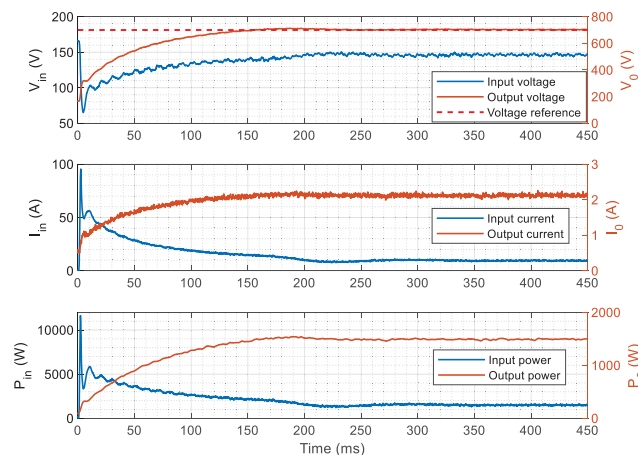


Figure 7: I/O signals of FIBC in stand alone mode : voltages:  $V_{\text{in}}$ ,  $V_0$ ; currents:  $I_{\text{in}}$ ,  $I_0$ ; powers:  $P_{\text{in}}$ ,  $P_0$ . 3 dB filtering option set at each scope channel.



In a second step, the FIBC converter was tested as part of the SWECS test bench, piloted by active and reactive P/PI currents controllers, which were first theoretically optimised as previously shown, then fine tuned in the real setup. This results in the following gains values :  $k_{p2}=300$ ,  $k_{i1}=474$  and  $k_{p1}=1.5$ . In parallel, the reference value of the DC-Link voltage ( $V_0$ ) is set at 700 V so as to enable power injection at 400 Vrms. Figure 8 shows the DC-Link voltage behaviour, along with the injected active power (the reactive power reference value being nul), this at varying input voltage ( $V_{in}$ ). One can observe the good stability of  $V_0$  with respect to  $V_{in}$  and to the injected active power into the grid, regardless some gaps that appear between real and reference powers due to the hardware.

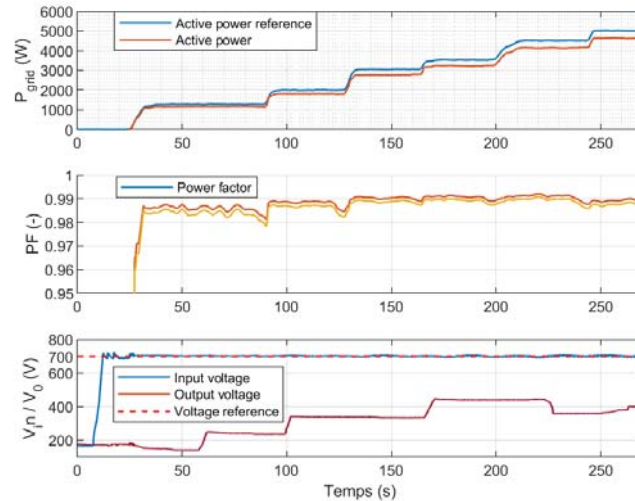


Figure 8: SWECS dynamic behaviour.  $P_{grid}/Q_{rid}$  : injected active/reactive power;  $V_{in}/V_0$  : input/output voltages of the FIBC.

## 6. CONCLUSION

In this paper has been proposed an alternative topology for small wind power conversion systems, in which a four phases FIBC boost converter has been used along with a diode rectifier, in order to replace the VSR of the conventional back-to-back topology. The FIBC converter has been designed, prototyped and tested. Experimental results confirms the good efficacy of output voltage and phases currents controls, and just as important, a very high efficiency. An experimental study has also been successfully conducted at the SWECS level, with power injection into the utility grid. The proposed topology bears a good potential to improve efficiency and compactness of the conventional one.

## ACKNOWLEDGMENT

The authors would like to thank those students of the High school of engineering and architecture, Fribourg, who actively participated to the laboratory work related to this paper.

## REFERENCES

- [1] Kabalo, M & Co. Experimental validation of high-voltage-ratio low-input-current-ripple converters for hybrid fuel cell supercapacitor systems. IEEE Transactions on Vehicular Technology 2012, 61:3430-3440.
- [2] Bühler, H. Réglage par mode de glissement. Lausanne, Switzerland : Presses polytechniques romandes, 1986.
- [3] Capone, M. Chaîne électromécanique à haut rendement pour la petite éolienne. MSc Deepening Project, College of Engineering and Architecture Fribourg, University of Applied Sciences HES-SO, Fribourg, Switzerland, 2018.
- [4] Islam, Md & Co. Power converters for wind turbines: current and future development. In: Mendez-Vilas A, editor. Materials and Processes for Energy: Communicating Current Research and Technological Developments. Spain: Formatex Research Centre, 2013, pp.559–571.
- [5] El Hawary, M R & Co. Principles of Electric Machines with Power Electronic Applications. IEEE Press : A John Wiley and sons Inc;2002.
- [6] Reznik, A & Co. LCL Filter design and performance analysis for grid-interconnected systems. IEEE transactions on industry applications 2014, 50(2):1225-1232.